

# Observation of Terahertz Vibrations in the Nitrogenase FeMo Cofactor by Femtosecond Pump–Probe Spectroscopy\*\*

Ines Delfino, Giulio Cerullo, Salvatore Cannistraro, Cristian Manzoni, Dario Polli, Christie Dapper, William E. Newton, Yisong Guo, and Stephen P. Cramer\*

Human reliance on synthetic nitrogen fertilizers produced in the Haber–Bosch ammonia synthesis process has a host of undesirable consequences,<sup>[1]</sup> including dead zones from eutrophication, contributions to acid rain and greenhouse gases, and the consumption of large quantities of natural gas and coal.<sup>[2]</sup> Increased understanding of the alternative route, biological nitrogen fixation, could lead to better options for the delivery of fixed nitrogen to crop plants.<sup>[3,4]</sup> In any case, it would be instrumental in solving one of the longstanding questions in catalysis: How does nature reduce dinitrogen to ammonia at low temperatures and at atmospheric pressure?

One of the best-studied biological nitrogen-fixation systems is the Mo-dependent nitrogenase (N<sub>2</sub>ase) from *Azotobacter vinelandii*.<sup>[3–5]</sup> The active site of this enzyme employs a MoFe<sub>7</sub>S<sub>9</sub>X-homocitrate “FeMo-cofactor”, where “X” is an unidentified interstitial light atom, and this cluster is extractable into organic solvents as the small molecule “FeMoco”.<sup>[6–9]</sup> Dramatic progress has been made recently using electron nuclear double resonance (ENDOR) of nitrogenase mutants under special conditions to observe nitrogenous intermediates at various states of reduction.<sup>[10–14]</sup> However, techniques are still needed to characterize nitrogenase from other points of view, preferably on short time scales and in solution. In this work, as a prelude to measure-

ments on complex samples, we have investigated *N*-methylformamide (NMF) solutions of isolated FeMoco using impulsive coherent vibrational spectroscopy (ICVS). The results are compared to those from nuclear resonance vibrational spectroscopy (NRVS),<sup>[15,16]</sup> and the combination of data from both of these techniques allows a more comprehensive description of FeMoco vibrational activity.

In the ICVS experiment, an ultrashort pump laser pulse, resonant with the sample absorption, promotes a small fraction of the molecules to an electronic excited state. A probe pulse delayed by time  $\tau$  measures the time-dependent differential transmission ( $\Delta T/T$ ) signal. If the pump pulse duration is significantly shorter than the periods of the vibrations of interest, then a coherent vibrational wave packet can be formed in the excited and/or in the ground electronic states. Periodic motion of this packet along displaced bond coordinates will modulate, by means of Franck–Condon factors, the molecular absorption. Fourier transformation of the oscillatory component of the time-dependent  $\Delta T/T$  signal yields vibrational frequencies coupled to the electronic transition for the chromophore under study. To date, ICVS has been applied to the study of several biochemical systems, including heme proteins,<sup>[17–19]</sup> green fluorescent protein,<sup>[20]</sup> blue copper proteins such as azurin,<sup>[21]</sup> plastocyanin,<sup>[22–25]</sup> and umecyanin,<sup>[26]</sup> and the Fe(Cys)<sub>4</sub> site in the electron-transfer protein rubredoxin.<sup>[27]</sup>

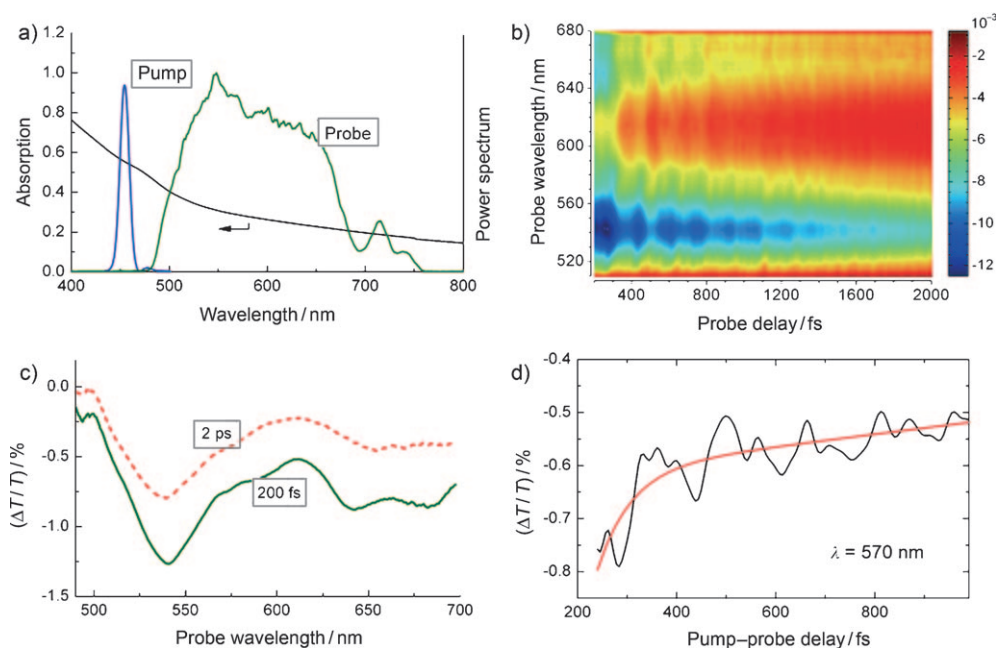
In our ICVS experiments, a benzenethiolate-treated FeMoco solution was pumped by 15 fs pulses centered at 450 nm, and probed by sub-10 fs pulses with a broadband spectrum spanning the 500–700 nm range.<sup>[28,29]</sup> Figure 1a shows the steady-state absorption spectrum for this FeMoco solution, together with the spectra of the pump and probe pulses. The relatively featureless FeMoco absorption spectrum is one indicator of sample integrity, because air-oxidized FeMoco exhibits a variety of distinct features in its visible spectrum.<sup>[30]</sup> No changes in the absorption spectrum were observed during the ICVS experimental sessions. Over a period of several weeks of storage, the sample bleached and a distinct absorption band grew in at 470 nm (see the Supporting Information), indicating the presence of air-oxidized FeMoco.<sup>[30]</sup> These observations indicate that the integrity of the sample was maintained during the period when the ICVS measurements were conducted.

Figure 1b shows the 2D differential transmission map  $\Delta T/T(\lambda, \tau)$  following excitation at 450 nm.  $\Delta T/T$  spectra at two different time delays are shown in Figure 1c, whereas a typical dynamics together with an exponential fit is reported in Figure 1d. The response is strongest around 540 nm, but absorption changes are clear out to 700 nm. The raw pump–

[\*] Dr. I. Delfino, Prof. S. Cannistraro  
Biophysics & Nanoscience Centre, CNISM  
Facoltà di Scienze, Università della Tuscia (Italy)  
Prof. G. Cerullo, Dr. C. Manzoni, Dr. D. Polli  
IFN-CNR, Dipartimento di Fisica  
Politecnico di Milano (Italy)  
Dr. C. Dapper, Prof. W. E. Newton  
Department of Biochemistry  
Virginia Polytechnic Institute & State University (USA)  
Dr. Y. Guo, Prof. S. P. Cramer  
Department of Applied Science, University of California  
Davis, CA 95616 (USA)  
E-mail: spjcramer@ucdavis.edu  
Prof. S. P. Cramer  
Physical Biosciences Division, Lawrence Berkeley National  
Laboratory, Berkeley, CA 94720 (USA)

[\*\*] This work was funded by the NIH (GM-65440 and EB-001962 to S.P.C.), the NSF (CHE-0745353 to S.P.C.), and the DOE Office of Biological and Environmental Research (S.P.C.). Use of APS is supported by DOE Office of Basic Energy Sciences, Office of Science. SPring-8 is funded by JASRI.

Supporting information for this article (including protein purification and FeMoco isolation procedures, details of femtosecond pump probe experiment, and the absorption spectrum before and after data collection) is available on the WWW under <http://dx.doi.org/10.1002/anie.200906787>.



**Figure 1.** a) Absorption spectrum for benzenethiolate FeMoco (solid black line); pump spectrum at 450 nm and the broadband probe used for ICVS experiments are also shown; b) 2D differential transmission spectrum  $\Delta T/T(\lambda, \tau)$  spectrum following excitation at 450 nm; c)  $\Delta T/T$  spectra recorded at  $\tau = 200$  fs and 2 ps; d)  $\Delta T/T$  dynamics at a probe wavelength of 570 nm together with an exponential fit (red curve).

probe data present a strong signal at zero time delay that lasts for about 100 fs. This can be ascribed to a nonresonant response of the solvent.<sup>[17,25,26]</sup> In order to remove the effects of this artifact, we limited our analysis to time delays longer than 200 fs. In all cases, the traces show an exponential decay that is modulated by clearly visible oscillations. The negative  $\Delta T/T$  signal (photoinduced absorption) is most likely due to a transition from the photoexcited level to a higher excited state, with oscillator strength greater than the ground-state transition. By fitting the  $\Delta T/T$  data with an exponential decay plus an offset, we found that the population of the electronic excited state decays with a time constant of roughly 200 fs. This time constant is similar to the 230–300 fs values recently observed in rubredoxin<sup>[27]</sup> and in a [2Fe-2S] ferredoxin,<sup>[31]</sup> suggesting that rapid nonradiative coupling between excited and ground states is a general characteristic of Fe-S chromophores.

The trace in Figure 1d shows that the  $\Delta T/T$  signal is modulated by a complex oscillatory signal, assigned to vibrational coherence created by the very short pump pulses.<sup>[23]</sup> The oscillations occur at frequencies that correspond to the vibrational modes coupled to the electronic transition for the chromophore under study, and the Fourier transform of these oscillations is similar to the resonance Raman spectrum.<sup>[32]</sup> Figure 2a (upper trace) shows as a representative example the oscillatory component of the FeMoco signal at a probe wavelength of 570 nm, as obtained after subtraction of the exponential decay component. These oscillations are exponentially damped with a time constant of approximately 1 ps. The corresponding Fourier spectrum of the data is shown in Figure 2b (upper trace). In order to distinguish between FeMoco and solvent features, we

recorded the responses for a solvent blank, and these are also illustrated in Figure 2 (lower traces).

The ICVS spectrum for FeMoco in NMF is particularly simple—a dominant band at 215  $\text{cm}^{-1}$  and a moderate peak at 420  $\text{cm}^{-1}$ . In comparison, the NMF solvent spectrum has no structure at these values, hence these two main bands can be unambiguously assigned to the presence of FeMoco. The FeMoco spectrum also contains weak features between the main peaks, at 265, 293, 319, and 381  $\text{cm}^{-1}$ . It also has low-energy peaks around 66 and 95  $\text{cm}^{-1}$  and a very weak high-energy feature at 670  $\text{cm}^{-1}$ .

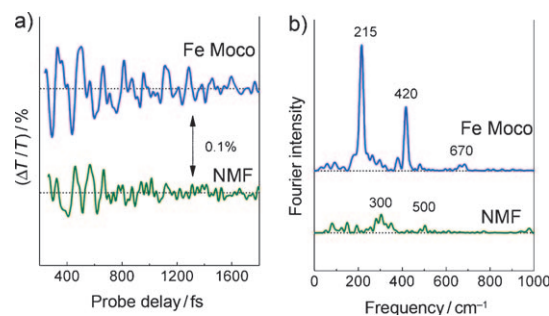


**Figure 2.** a) Oscillatory components of the pump-probe response probed at 570 nm after excitation at 450 nm. b) Corresponding Fourier transforms for FeMoco solution in NMF (top) and NMF solvent blank (bottom).

Although definitive assignment of the strong band at 420  $\text{cm}^{-1}$  must await expensive isotopic labeling experiments, we note that many [2Fe-2S] clusters in model compounds and ferredoxins have asymmetric ( $b_{2u}$ ) Fe-S stretching modes in this region.<sup>[33,34]</sup> Similarly, many [4Fe-4S] clusters in models and ferredoxins have Fe-S stretching modes in the 265–381  $\text{cm}^{-1}$  range where we see the weaker FeMoco bands.<sup>[35,36]</sup> Thus, all of the features from 265 to 420  $\text{cm}^{-1}$  are consistent with Fe-S stretching modes similar to those seen in other Fe-S clusters.

We now discuss the dominant band at 215  $\text{cm}^{-1}$ , which turns out to be the unique feature in the spectrum. We know from previous NRVS simulations, as well as the large body of resonance Raman studies on Fe-S clusters, that the 200  $\text{cm}^{-1}$  region derives from normal modes that are primarily breathing and bending in character.<sup>[15,16]</sup> To assign this mode, we

compare the ICVS data with previous measurements on various  $^{57}\text{FeMoco}$  samples using NRVS<sup>[15,16]</sup> (Figure 3). In making this comparison, of course we cannot expect the same

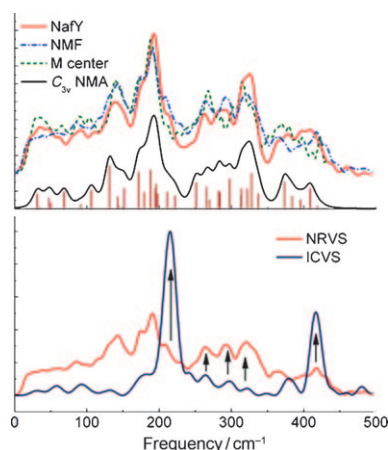


**Figure 3.** Upper panel: NRVS for three different forms of FeMoco, compared with an empirical simulation with lines corresponding to individual normal modes.  $C_{3v}$  NMA: normal mode analysis for a simplified  $C_{3v}$  model. The three FeMoco forms are: NaFY: FeMoco bound to the small protein NaFY; NMF: isolated FeMoco in NMF solution; M center: FeMo cofactor in intact nitrogenase.<sup>[15,16]</sup> Lower panel: Comparison of ICVS and NRVS spectra for FeMoco in NMF. Arrows denote the positions of the main modes identified by ICVS.

intensities, because ICVS and NRVS have very different selection rules—the latter technique being sensitive only to  $^{57}\text{Fe}$  motion. Mismatches between NRVS and resonance Raman intensities have been observed and discussed for the  $\text{FeS}_4$  breathing mode in rubredoxin,<sup>[37]</sup> the out-of-phase  $\text{Fe}_2\text{S}_6$  breathing mode in 2Fe ferredoxins,<sup>[34]</sup> and the symmetric breathing mode at  $\approx 338\text{ cm}^{-1}$  in 4Fe ferredoxins.<sup>[36]</sup> Furthermore, the ICVS measurements were performed on a natural-abundance FeMoco sample at room temperature in NMF, whereas the NRVS data were obtained for frozen  $^{57}\text{FeMoco}$  samples at about 100 K either in a protein matrix or NMF. Despite these caveats, there are some correspondences between the spectra obtained with the two different techniques.

In the NRVS data sets, the overall maximum is at approximately  $190\text{ cm}^{-1}$ , but in each case there is also a peak or clear shoulder on the high-energy side between roughly 210 and  $230\text{ cm}^{-1}$ . Using the force field developed to fit the NRVS data,<sup>[15,16]</sup> a normal mode analysis with a simplified  $C_{3v}$  model predicts a totally symmetric breathing mode at  $222\text{ cm}^{-1}$ , and a pair of E symmetry modes at  $211\text{ cm}^{-1}$ . The motion in these modes is shown in Figure 4, along with the other symmetric breathing mode at  $190\text{ cm}^{-1}$  and an E symmetry Fe–S stretching mode predicted at approximately  $417\text{ cm}^{-1}$ .

In summary, using the ICVS technique, we have identified two key vibrational frequencies for FeMoco, at approximately 215 and  $430\text{ cm}^{-1}$ . The  $215\text{ cm}^{-1}$  band is in a region less commonly probed in resonance Raman studies of Fe–S clusters and above the strongest NRVS features. By compar-

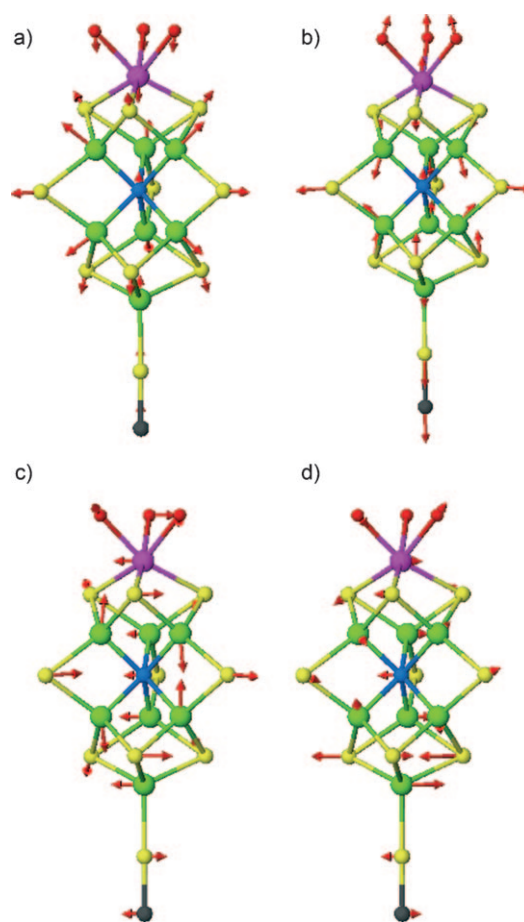


**Figure 4.** Calculated modes for a FeMoco model with  $C_{3v}$  symmetry. a) totally symmetric  $A_1$  breathing mode at  $190\text{ cm}^{-1}$ , b) totally symmetric  $A_1$  breathing mode at  $225\text{ cm}^{-1}$ , c) E symmetry breathing mode at  $213\text{ cm}^{-1}$ , d) E symmetry Fe–S stretching mode at  $417\text{ cm}^{-1}$ .

ing the ICVS spectra to NRVS data and normal mode analyses, we assign the low-frequency mode to A and/or E symmetry cluster breathing modes. Such breathing modes should be useful diagnostics for nitrogenase chemistry, because they are expected to be sensitive to the binding of substrates and inhibitors to any of the iron centers in the central prism. In contrast, the high-frequency Fe–S stretching mode at  $417\text{ cm}^{-1}$  should be sensitive to the redox state of FeMoco. Because the ICVS experiment is sensitive to both the pump and probe wavelengths, additional experiments should find conditions that enhance other FeMoco normal modes. Using ICVS it should be possible to observe chemical changes in the protein-bound FeMo cofactor, thus shedding light on the nitrogenase catalytic mechanism. There is obviously great potential for application of this technique to studies of other Fe–S enzymes on very short time scales.

Received: December 2, 2009

Published online: ■■■■■, 2010

**Keywords:** bioinorganic chemistry · nitrogenases · pump–probe spectroscopy · vibrational spectroscopy

- [1] J. N. Galloway, A. R. Townsend, J. W. Erisman, M. Bekunda, Z. Cai, J. R. Freney, L. A. Martinelli, S. P. Seitzinger, M. A. Sutton, *Science* **2008**, *320*, 889.
- [2] N. Nosengo, *Nature* **2003**, *425*, 894.
- [3] J. W. Peters, R. K. Szilagyi, *Curr. Opin. Chem. Biol.* **2006**, *10*, 101.
- [4] W. E. Newton, *Nitrogen Fixation: Origins, Applications, and Research Progress, Vol. 1–7*, Springer, The Netherlands, **2004–2008**.
- [5] D. C. Rees, F. A. Tezcan, C. A. Haynes, M. Y. Walton, S. Andrade, O. Einsle, J. B. Howard, *Philos. Trans. R. Soc. London Ser. A* **2005**, *363*, 971.
- [6] V. Shah, W. Brill, *Proc. Natl. Acad. Sci. USA* **1977**, *74*, 3249.
- [7] S. S. Yang, W. H. Pan, G. D. Friesen, B. K. Burgess, J. L. Corbin, E. I. Stiefel, W. E. Newton, *J. Biol. Chem.* **1982**, *257*, 8042.
- [8] D. A. Wink, P. A. McLean, Alison B. Hickman, W. H. Orme-Johnson, *Biochemistry* **1989**, *28*, 9407.
- [9] C. J. Pickett, K. A. Vincent, S. K. Ibrahim, C. A. Gormal, B. E. Smith, S. P. Best, *Chem. Eur. J.* **2003**, *9*, 76.
- [10] B. M. Barney, M. Laryukhin, R. Y. Igarashi, H.-I. Lee, P. C. D. Santos, T.-C. Yang, B. M. Hoffman, D. R. Dean, L. C. Seefeldt, *Biochemistry* **2005**, *44*, 8030.
- [11] B. M. Barney, T.-C. Yang, R. Y. Igarashi, P. C. D. Santos, M. Laryukhin, H.-I. Lee, B. M. Hoffman, D. R. Dean, L. C. Seefeldt, *J. Am. Chem. Soc.* **2005**, *127*, 14960.
- [12] B. M. Barney, D. Lukoyanov, T. C. Yang, D. R. Dean, B. M. Hoffman, L. C. Seefeldt, *Proc. Natl. Acad. Sci. USA* **2006**, *103*, 17113.
- [13] D. Lukoyanov, B. M. Barney, D. R. Dean, L. C. Seefeldt, B. M. Hoffman, *Proc. Natl. Acad. Sci. USA* **2007**, *104*, 1451.
- [14] B. M. Barney, J. McClead, D. Lukoyanov, M. Laryukhin, T.-C. Yang, Dennis R. Dean, Brian M. Hoffman, L. C. Seefeldt, *Biochemistry* **2007**, *46*, 6784.
- [15] Y. Xiao, K. Fischer, M. C. Smith, W. Newton, D. A. Case, S. J. George, H. Wang, W. Sturhahn, E. E. Alp, J. Zhao, Y. Yoda, S. P. Cramer, *J. Am. Chem. Soc.* **2006**, *128*, 7608.
- [16] S. J. George, R. Y. Igarashi, Y. Xiao, J. A. Hernandez, M. Demuez, D. Zhao, Y. Yoda, P. W. Ludden, L. M. Rubio, S. P. Cramer, *J. Am. Chem. Soc.* **2008**, *130*, 5673.
- [17] L. Zhu, P. Li, M. Huang, J. T. Sage, P. M. Champion, *Phys. Rev. Lett.* **1994**, *72*, 301.
- [18] F. Rosca, A. T. N. Kumar, D. Ionascu, T. Sjodin, A. A. Demidov, P. M. Champion, *J. Chem. Phys.* **2001**, *114*, 10884.
- [19] F. Gruia, D. Ionascu, M. Kubo, X. Ye, J. Dawson, R. L. Osborne, S. G. Sligar, I. Denisov, A. Das, T. L. Poulos, J. Terner, P. M. Champion, *Biochemistry* **2008**, *47*, 5156.
- [20] R. A. G. Cinelli, V. Tozzini, V. Pellegrini, F. Beltram, G. Cerullo, M. Zavelani-Rossi, S. De Silvestri, M. Tyagi, M. Giacca, *Phys. Rev. Lett.* **2001**, *86*, 3439.
- [21] T. Cimei, A. R. Bizzarri, S. Cannistraro, G. Cerullo, S. D. Silvestri, *Chem. Phys. Lett.* **2002**, *362*, 497.
- [22] M. D. Edington, W. M. Diffey, W. J. Doria, R. E. Riter, W. F. Beck, *Chem. Phys. Lett.* **1997**, *275*, 119.
- [23] L. D. Book, D. C. Arnett, H. Hu, N. F. Scherer, *J. Phys. Chem. A* **1998**, *102*, 4350.
- [24] S. Nakashima, Y. Nagasawa, K. Seike, T. Okada, M. Sato, T. Kohzuma, *Chem. Phys. Lett.* **2000**, *331*, 396.
- [25] T. Cimei, A. R. Bizzarri, G. Cerullo, S. D. Silvestri, S. Cannistraro, *Biophys. Chem.* **2003**, *106*, 221.
- [26] I. Delfino, C. Manzoni, K. Sato, C. Dennison, G. Cerullo, S. Cannistraro, *J. Phys. Chem. B* **2006**, *110*, 17252.
- [27] M.-L. Tan, A. R. Bizzarri, Y. Xiao, S. Cannistraro, T. Ichiye, C. Manzoni, G. Cerullo, M. W. W. Adams, J. Francis E. Jenney, S. P. Cramer, *J. Inorg. Biochem.* **2007**, *101*, 375.
- [28] C. Manzoni, D. Polli, G. Cerullo, *Rev. Sci. Instrum.* **2006**, *77*, 023103.
- [29] D. Polli, L. Lüer, G. Cerullo, *Rev. Sci. Instrum.* **2007**, *78*, 103108.
- [30] W. E. Newton, S. F. Gheller, B. Hedman, K. O. Hodgson, S. M. Lough, J. W. McDonald, *Eur. J. Biochemistry* **1986**, *159*, 111.
- [31] P. Kim, D. Larsen, J. Meyer, S. P. Cramer, **2010**, manuscript in preparation.
- [32] A. B. Myers, *Acc. Chem. Res.* **1997**, *30*, 519.
- [33] M. C. Smith, Y. Xiao, H. Wang, S. J. George, D. Coucovanis, M. Koutmos, W. Sturhahn, E. E. Alp, J. Zhao, S. P. Cramer, *Inorg. Chem.* **2005**, *44*, 5562.
- [34] Y. Xiao, M.-L. Tan, T. Ichiye, H. Wang, Y. Guo, M. C. Smith, J. Meyer, W. Sturhahn, E. E. Alp, J. Zhao, Y. Yoda, S. P. Cramer, *Biochemistry* **2008**, *47*, 6612.
- [35] Y. Xiao, M. Koutmos, D. A. Case, D. Coucovanis, H. Wang, S. P. Cramer, *Dalton Trans.* **2006**, 2192.
- [36] D. Mitra, V. Pelmentschikov, Y. Guo, D. A. Case, H. Wang, W. Dong, F. E. Jenney Jr., M. W. W. Adams, S. P. Cramer, *Biochemistry* **2010**, submitted.
- [37] Y. Xiao, H. Wang, S. J. George, M. C. Smith, M. W. W. Adams, J. Francis E. Jenney, W. Sturhahn, E. E. Alp, J. Zhao, Y. Yoda, A. Dey, E. I. Solomon, S. P. Cramer, *J. Am. Chem. Soc.* **2005**, *127*, 14596.

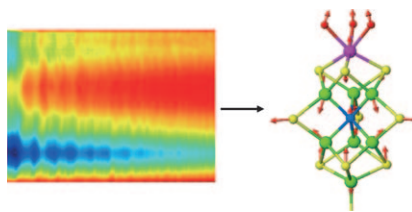
## Communications



### Pump-Probe Spectroscopy

I. Delfino, G. Cerullo, S. Cannistraro,  
C. Manzoni, D. Polli, C. Dapper,  
W. E. Newton, Y. Guo,  
S. P. Cramer\* ————— ■■■■-■■■■

Observation of Terahertz Vibrations in the  
Nitrogenase FeMo Cofactor by  
Femtosecond Pump-Probe Spectroscopy



**Pump it up!** The FeMo cofactor (see picture) has resisted characterization by resonance Raman spectroscopy. Impulsive coherent vibrational spectroscopy may be an alternative probe of its dynamics. A 15 fs visible laser pulse pumped the sample to an excited electronic state, and a second  $< 10$  fs pulse probed the change in transmission as a function of the time delay.